Energetics, structure, mechanical and vibrational properties of single-walled carbon nanotubes

Guanghua Gao, Tahir Çağın† and William A Goddard III

Materials and Process Simulation Center, Beckman Institute (139-74), Division of Chemistry and Chemical Engineering, California Institute of Technology, Pasadena, CA 91125, USA

Abstract. In this paper, we present extensive molecular mechanics and molecular dynamics studies on the energy, structure, mechanical and vibrational properties of single-wall carbon nanotubes. In our study we employed an accurate interaction potential derived from quantum mechanics. We explored the stability domains of circular and collapsed cross section structures of armchair (n, n), zigzag $(n, 0)$, and chiral $(2n, n)$ isolated single-walled carbon nanotubes (SWNTs) up to a circular cross section radius of 170 Å. We have found three different stability regions based on circular cross section radius. Below 10 Å radius only the circular cross section tubules are stable. Between 10 and 30 Å both circular and collapsed forms are possible, however, the circular cross section SWNTs are energetically favorable. Beyond 30 Å (crossover radius) the collapsed form becomes favorable for all three types of SWNTs. We report the behavior of the SWNTs with radii close to the crossover radius $((45, 45), (80, 0), (70, 35))$ under uniaxial compressive and tensile loads. Using classical thin-plane approximation and variation of strain energy as a function of curvature, we calculated the bending modulus of the SWNTs. The calculated bending moduli are $\kappa_{(n,n)} = 963.44$ GPa, $\kappa_{(n,0)} = 911.64$ GPa, and $\kappa_{(2n,n)} = 935.48$ GPa. We also calculated the interlayer spacing between the opposite sides of the tubes and found $d_{(n,n)} = 3.38$ Å, $d_{(2n,n)} = 3.39$ Å, and $d_{(n,0)} = 3.41$ Å. Using an enthalpy optimization method, we have determined the crystal structure and Young's modulus of (10,10) armchair, $(17, 0)$ zigzag and $(12, 6)$ chiral forms (which have similar diameter as (10,10)). They all pack in a triangular pattern in two dimensions. Calculated lattice parameters are $a_{(10,10)} = 16.78$ Å, $a_{(17,0)} = 16.52$ Å and $a_{(12,6)} = 16.52$ Å. Using the second derivatives of potential we calculated Young's modulus along the tube axis and found $Y_{(10,10)} = 640.30$ GPa, $Y_{(17,0)} = 648.43$ GPa, and $Y_{(12,6)} = 673.94$ GPa. Using the optimized structures of (10, 10), (12, 6) and (17, 0), we determined the vibrational modes and frequencies. Here, we report the highest in-plane mode, compression mode, breathing mode, shearing mode and relevant cyclop mode frequencies.

M This article features multimedia enhancements available from the abstract page in the online journal; see `http://www.iop.org`.

1. Introduction

Carbon nanotubes were discovered in 1991 by Iijima of NEC corporation [1]. Since then, efforts in synthesis, characterization and theoretical investigation on nanotubes have grown exponentially. This is mostly due to their perceived novel mechanical and electronic properties and their tremendous potential for future technological applications. In 1993, the simplest kind of carbon nanotubes, single-walled carbon nanotubes (SWNTs), were discovered independently by the Iijima group [2] and an IBM team headed by Bethune [3]. These SWNTs can be regarded as a rolled-up graphite sheet in cylindrical form.

† Author to whom all correspondence to be addressed.

Some specific defect-free forms of these SWNTs show remarkable mechanical properties and metallic behavior [4]. These materials present tremendous potential as components for use in nano-electronic and nano-mechanical device applications or as structural elements in various devices.

Thess and co-workers [4] later produced crystalline 'ropes' of metallic carbon nanotubes with 100–500 SWNTs bundled into a two-dimensional triangular lattice. These tightly bundled linear 'ropes' are expected to have remarkable mechanical properties, as well as superior electronic and magnetic properties. Various levels of studies were performed on the properties of the SWNTs, including use of classical molecular mechanics (MM),

lattice dynamics (LD), molecular dynamics (MD), tight binding and *ab initio* level quantum mechanical (QM) methods [5–18]. Robertson *et al* carried out first studies on the structure and energetics of isolated small-diameter SWNTs [13]. More recent theoretical studies include, behavior of nanotubes under high-rate tensile strain and fracture [14], size-dependent resonance Raman scattering [15] in nanotubes, mechanical behavior of SWNT under compression using MD [16], and a pioneering study on the structural flexibility of carbon nanotubes using HREM and atomistic simulations addressing the role of van der Waals radii reported by Tersoff and co-workers [17, 18].

In this paper, we present a detailed study of the energetics, structures, and mechanical properties of SWNT with different radius and chirality (armchair (n, n), chiral $(2n, n)$, and zigzag $(n, 0)$). We used an accurate force field, derived through QM calculations, to represent the interactions between the carbon atoms [19]. These interaction potentials were used earlier in studying structure, mechanical and vibrational properties of graphite, various fullerenes and intercalated compounds of fullerenes [20] and nanotubes [21]. In our studies, we employed classical MD and molecular mechanics methods as implemented in MPSim, a massively parallel program for materials simulations [22]. MD runs are performed to anneal the structures, whereas molecular mechanics, energy and/or enthalpy minimization, are applied at the end of the annealing cycle to obtain the final optimized structures. Using the analytical second derivatives of the potential energy, we also calculate the vibrational modes and frequencies of three kinds of nanotube bundles, $(10, 10)$ arm chair, $(17, 0)$ zigzag and $(12, 6)$ chiral. These tubes have comparable cross section diameters, and are among the easiest to make.

2. Energetics and the stability of circular versus collapsed tubes

In order to assess mechanical stability of various SWNTs, we created three chiral forms ((n, n) armchair, $(n, 0)$ zigzag, and $(2n, n)$) with various diameters. For each form, we studied two sets of initial structures, (1) perfect circular cross section and (2) elongated or collapsed cross section. For the collapsed structures, the opposite walls in the middle section are within van der Waals distance and the shape at the two ends is close to circular with a diameter of $D \tilde{} 10.7$ Å. To mimic a long isolated nanotube, we imposed a periodic boundary condition along the c-axis (the tube direction). To eliminate the intertube interactions, we set the cell parameters a and b to 50 times the circular tube diameter. Energy and structural optimizations were carried out using MPSim. Figure 1 shows the strain energy per carbon atom versus the radius of its circular form. We put the two sets (collapsed and circular) with three chiral forms ((n, n) armchair, $(n, 0)$ zigzag, and $(2n, n)$) on the same plot. For all three forms, there are regions associated with two transition radii (R_1 and R_2). For tubes with 'circular' radius smaller than R_1, only the circular form is possible, the collapsed initial structure transformed to the circular form during the structural optimization. For
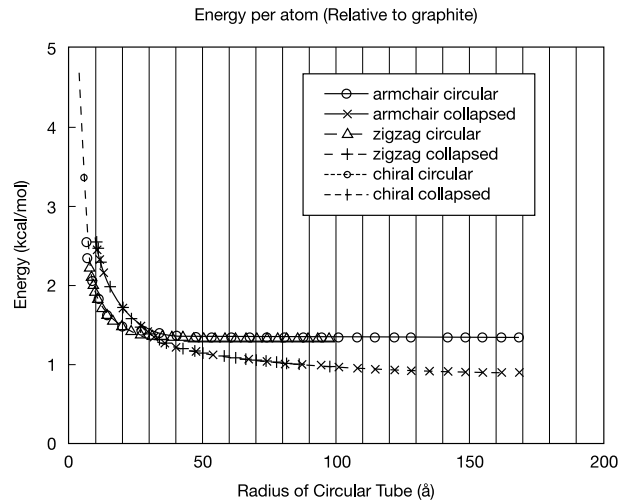

Figure 1. Energy per carbon atom (measured relative to graphite) of stable structures for (n, n) armchair, $(2n, n)$ chiral, and $(n, 0)$ zigzag SWNTs; R is the radius of the corresponding 'circular' form.

tubes with 'circular' radius between R_1 and R_2, there are two stable structures with the circular structure energetically more stable. For tubes with 'circular' radius larger than R_2, the collapsed form becomes energetically favored while the circular form becomes metastable. The structures and radii of the first transition are:

• (n, n) armchair: R_1 is between 10.77 Å of $(16, 16)$ and 11.44 Å of $(17, 17)$;

• $(2n, n)$ chiral: R_1 is between 10.28 Å of $(20, 10)$ and 11.31 Å of $(22, 11)$;

• $(n, 0)$ zigzag: R_1 is between 10.49 Å of $(27, 0)$ and 10.88 Å of $(28, 0)$.

The structures and the radii of the second transition are:

• (n, n) armchair: R_2 is between 29.62 Å of $(45, 45)$ and 30.30 Å of $(46, 46)$;

• $(2n, n)$ chiral: R_2 is between 29.82 Å of $(58, 29)$ and 30.85 Å of $(60, 30)$;

• $(n, 0)$ zigzag: R_2 is between 29.93 Å of $(77, 0)$ and 30.32 Å of $(78, 0)$.

Looking at the collapsed structures of various radii along tube axis, we found that they all have two circular (or elliptical) ends with a diameter D of $\tilde{} 10.5$ Å and a flat middle section. The inner wall distances in the flat region are close to 3.4 Å, which is very similar to the interlayer spacing of adjacent sheets in graphite crystals. The end sections are highly strained compared with the circular form, thus cost energy. In addition to zero strain energy, the flat region is further stabilized by interlayer van der Waals attractions. The relative strength of these two opposite forces dictates the two structural transformations. Shown in figure 2 are the optimized structures of armchair (n, n) tubes with collapsed initial structures viewed along the c-axis. The zigzag $(n, 0)$ and chiral $(2n, n)$ tubes are similar.

Based on the optimized structures and their energies of the circular form, we can model the basic energetics by approximating the tube as a membrane with a curvature $1/R$ and bending modulus of κ [23]. Assuming a as the
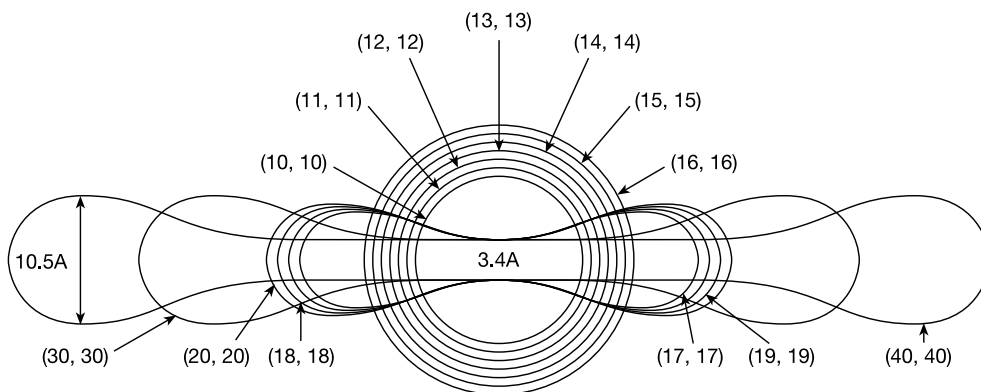
Figure 2. Cross sections of the optimum (n, n) tubes (started from the collapsed forms shown).
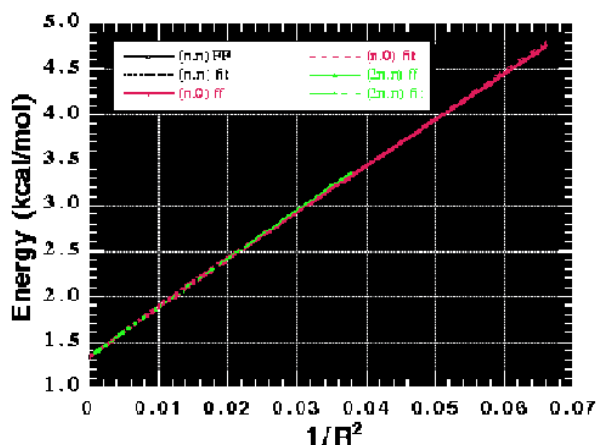

Figure 3. Strain energy as a function of tube radius.

thickness of tube wall, the elastic energy stored in a slab of width L, is given by

$$E_{\text{strain}} = \frac{\pi \kappa L a^2}{12R}.$$

The per atom energy can be written as

$$E_C = \frac{\pi \kappa L a^2}{12RN} + E_0$$

where N is the number of carbon atoms per slab and E_0 is the energy per carbon atom for tubes as $1/R$ goes to 0, i.e. flat sheets. Considering $N = 2\pi \rho L R$ the number of carbon atoms per unit area of tube wall, we have

$$E_C = \kappa \frac{a^2}{24\rho} \frac{1}{R^2} + E_0.$$

Setting $a = 3.335$ Å, the same as the spacing between two graphite sheets, $R_0 = 1.410$ Å, the C–C bond distance, we obtained $\kappa_{(n,n)} = 963.44$ GPa, $\kappa_{(n,0)} = 911.64$ GPa, and $\kappa_{(2n,n)} = 935.48$ GPa. These results are plotted against the theoretical estimates in figure 3.

The bending moduli of sheets with different chirality suggest that the transition radius depends on the chirality,
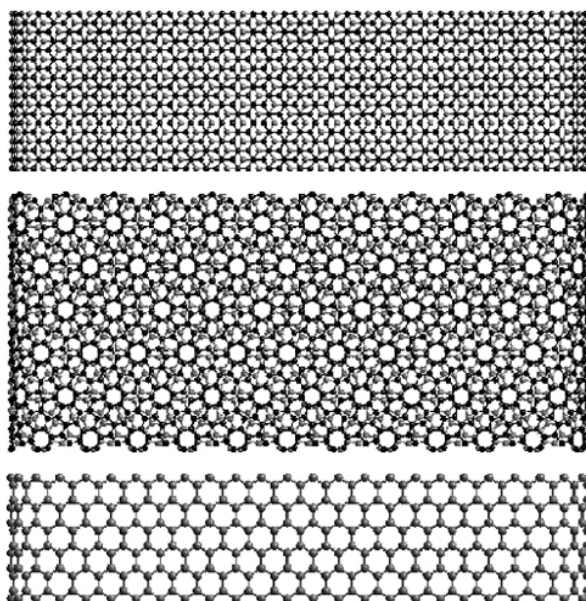

Figure 4. Side views of interlayer stacking patterns of: (*a*) $(30, 30)$ armchair; (*b*) $(50, 25)$ chiral and (*c*) $(50, 0)$ zigzag SWNTs.

with a $(2n, n)$ transition radius larger than that of $(n, 0)$ zigzag, but smaller than that of (n, n) armchair. That is what we expected, because the higher the bending modulus, the higher the strain energy. The (n, n) armchair has higher binding energy than that of $(2n, n)$, while the $(n, 0)$ zigzag has lower binding energy than that of $(2n, n)$. However, by examining the collapsed structures closely, we also found different interlayer stacking in the collapsed region. Figure 4 is the side views of the two attracting layers for three cases. The interlayer stacking patterns are different due to different chirality.

The interlayer distances also differ slightly, with $d_{(n,n)} = 3.38$ Å, $d_{(2n,n)} = 3.39$ Å, and $d_{(n,0)} = 3.41$ Å. Energetically, interlayer attraction of armchair is the best with a per atom energy $E = 0.7336$ kcal mol^{-1}, and stacking of the opposite walls is almost identical to the graphite stacking. The interlayer attraction in the zigzag form is the worst with a per atom energy $E = 0.7439$ kcal mol^{-1}, since the carbon atoms on different layers are lined up on top of each other. The attraction
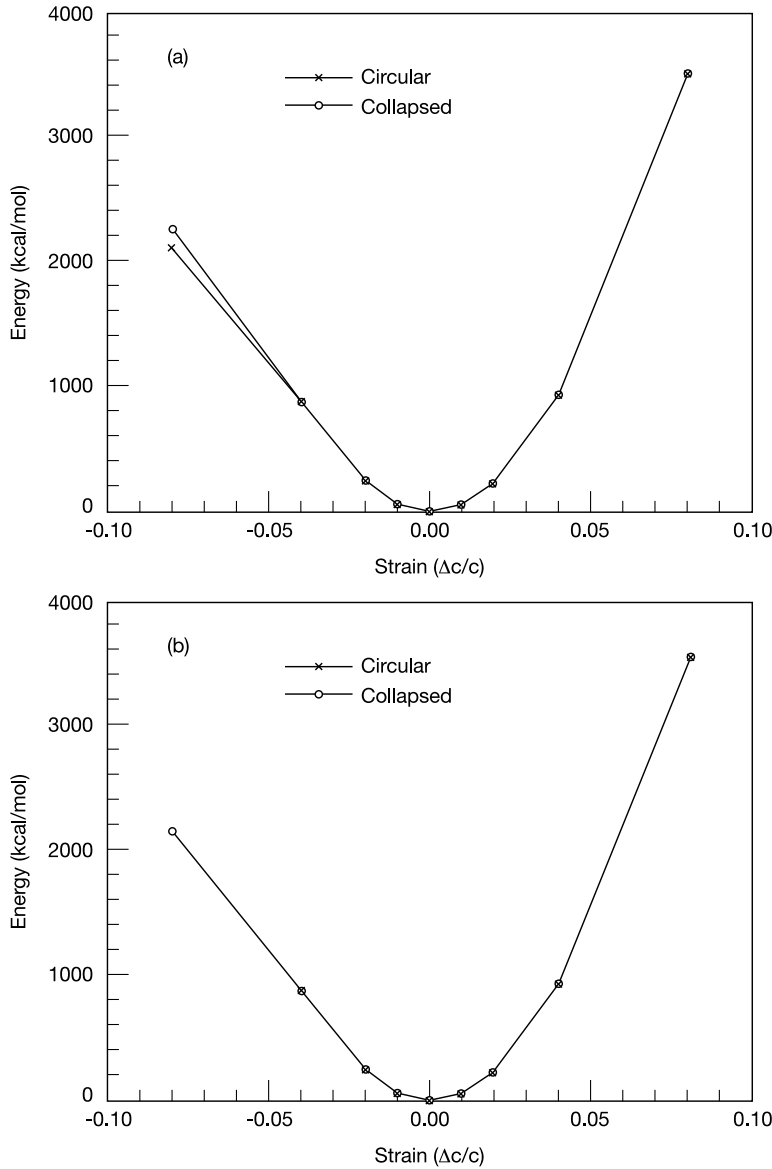
Figure 5. Strain energies, (*a*) strain energy versus strain for $(45, 45)$ armchair SWNT; (*b*) strain energy versus strain for $(80, 0)$ zigzag SWNT; (*c*) strain energy versus strain for $(70, 35)$ chiral SWNT.

energy per atom for the collapsed $(2n, n)$ chiral nanotube is in between the two. Overall, the two factors (bending modulus and van der Waals attraction) cancel out for different chirality, so that in terms of transition radius and the crossover radius, the size of the circular tube (radius) is the dominant factor in deciding the stable forms.

3. Stretching and compressing tubes at the crossover radius

In order to assess the tensile and compressive strength of the SWNTs, we also performed a series of compressive and tensile loading experiments by varying the c lattice parameter, along the tube axis. With respect to the optimum c lattice parameter, c_0, the strain can be defined as

$$\epsilon = \frac{\Delta c}{c}.$$

At the crossover radius, we calculated the energies of collapsed and circular tubes of $(45, 45)$, $(80, 0)$, and $(70, 35)$ under compression and tensions along tube axis. In figure 5(*a*), the armchair, figure 5(*b*), the zigzag, and figure 5(*c*), the chiral forms, we observe a nonlinear dependence on the strain.

The tubes are softer under compression due to the buckling effect. We present views along the tube axis and perpendicular to the tube axis in figure 6. Based on these energy versus strain curves, we also calculated 'elastic constants', the second derivative of energy with respect to applied strain, ϵ, along the tube axis, table 1.

4. Structure and mechanical properties of packed SWNT crystals

Among various conformations, the $(10, 10)$ armchair SWNT is the easiest to make. We studied the mechanical

187
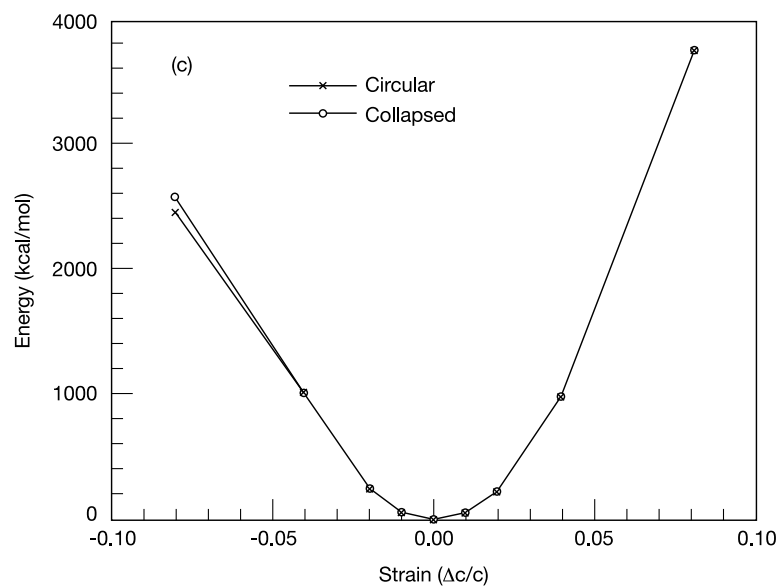
Figure 5. (Continued)
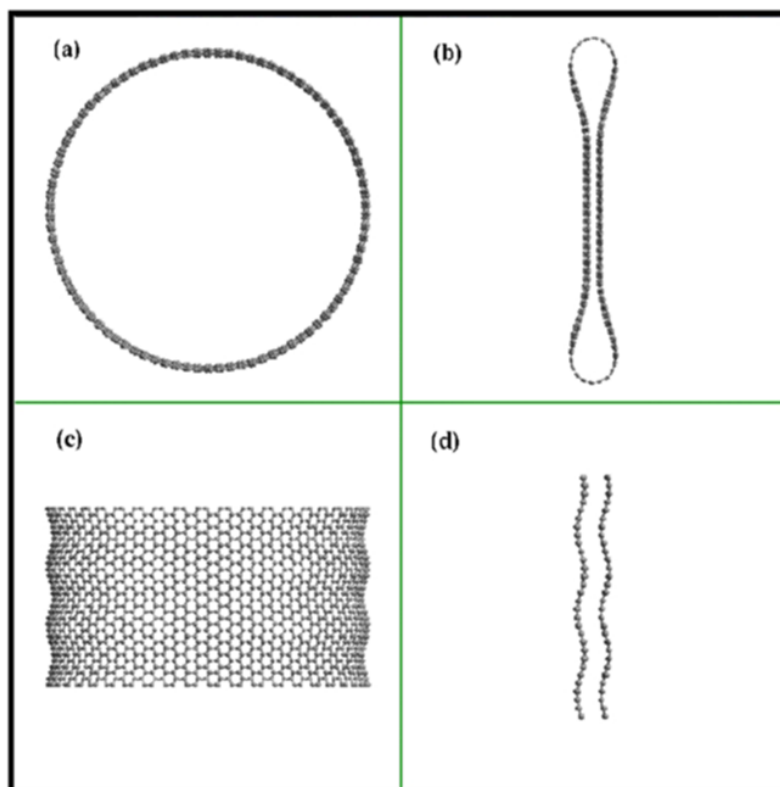
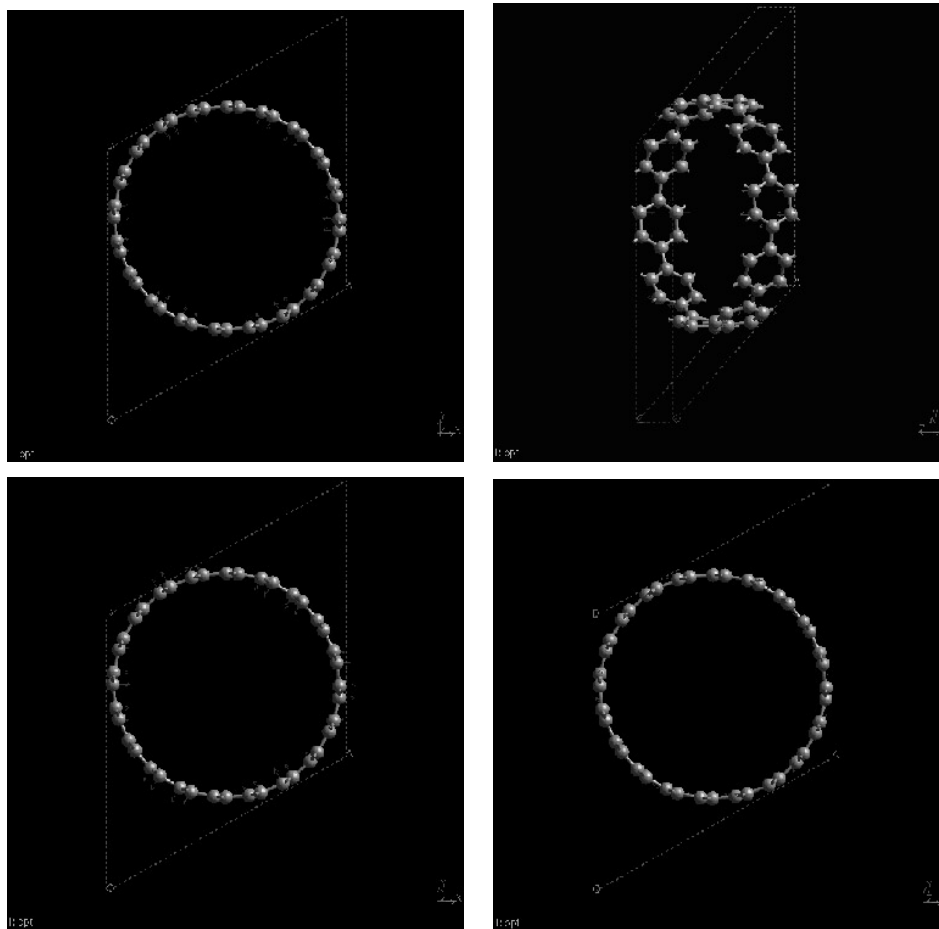**Figure 6.** Views of tubes perpendicular to and along tube axis.

Figure 7. Selected vibrational modes for (10, 10) tube, (*a*) Top left, uniform compression mode; (*b*) bottom left, shearing along tube mode; (*c*) top right, breathing mode (*d*) bottom right, cyclop mode.

M An MPEG movie of this figure is available from the article's abstract page in the online journal; see `http://www.iop.org`.

Table 2. The uniform compression (first row) and the highest in plane modes (second row) for (10, 10) SWNT.

(7,7)	(8,8)	(9,9)	(12,6)	(17,0)	(10,10)	(11,11)	(12,12)	(13,13)
261	231	207	202	188	186	168	152	138
1583	1584	1584	1585	1586	1584	1584	1584	1584

Table 1. Elastic modulus along the tube axis for circular and collapsed forms expressed in units of 10^5 kcal mol^{-1}.

	(45, 45)	(80, 0)	(70, 35)
Circular	6.2162	6.3965	6.7431
Collapsed	5.7351	5.9747	6.7105

properties of its bulk phase (10, 10) tube bundles. We also calculated the bulk properties of (17, 0) zigzag and (12, 6) chiral tubes, with cross section radii close to that of (10, 10) armchair tube. In the bulk phase we determine the specific packing, density, lattice parameters. MD and MM studies led to a triangular packing as the most stable form for all three forms. The triangular lattice

parameter for (10, 10) armchair is $a = 16.78$ Å with a density $\rho = 1.33$ g cm^{-3}. For the (17,0) zigzag, they are $a = 16.52$ Å and $\rho = 1.34$ g cm^{-3}. For the chiral form (12, 6), they are $a = 16.52$ Å and $\rho = 1.40$ g cm^{-3}. More importantly, we determined the Young's modulus along the tube axis for triangular-packed SWNTs using the second derivatives of the potential energy. They are $Y_{(10,10)} = 640.30$ GPa, $Y_{(17,0)} = 648.43$ GPa, and $Y_{(12,6)} = 673.49$ GPa, respectively. Normalized to carbon sheet these values are within a few per cent of the graphite bulk value.

5. Vibrational modes and frequencies of SWNTs

Using the second derivatives of the potential energy surface we calculated vibrational modes of a series of (n, n) tubes. The uniform compression and highest in-plane modes are

Table 3. Vibrational modes of (10, 10), (12, 6), and (17, 0) single-wall nanotubes. Breathing mode (B), shearing mode (S) and cyclops (C).

Mode	(10,10) B	S	C	(12,6) B	S	C	(17,0) B	S	C
1		111	242		122	265		113	247
		112	244		122	265		113	247
2	53	223	381	59	243	412	54	227	386
	53	223	381	59	243	412	54	227	386
3	49	333	524	57	364	566	50	341	530
	55	333	530	63	364	571	57	342	535
4	127	442	671	137	483	720	128	456	675
	127	442	671	137	483	720	129	456	676
5	147	549	805	168	600	850	149	570	806
	147	549	805	168	600	850	150	570	806
6	201	652	924	229	713	976	203	683	921
	226	652	925	249	713	977	227	683	921
7	262	750		299	819	1072	267	794	1017
	272	750		299	819	1072	267	794	1017
8	328	838		360	912	1136	327	901	1091
	330	838		360	912	1136	328	901	1091
9	375	909		396		379	1002	1140	
	381	909		400		385	1002	1140	
10	402	939		394		434			

listed in table 2 for $n = 7$ to 13. Among (n, n) tubes we focused on the (10, 10) tube crystal. We also calculated the vibrational frequencies and modes for the zigzag (17, 0) and chiral (12, 6) tube crystals due to their comparable tube radius to (10, 10). We listed the breathing, shearing and cyclop modes for these equivalent radius nanotubes in table 3. These results may be used to differentiate chiral tubes with comparable diameters. The uniform compression mode is also shown in figure 7(*a*) and occurs at 186 cm^{-1} for (10, 10), which is exactly the same as the experimental frequency [24]. In table 3 the B denotes the breathing mode as displayed in figure 7(*b*), S stands for shearing mode as in figure 7(*c*), and C stands for cyclops as in figure 7(*d*).

6. Concluding remarks

We presented a detailed study of structure, energetics and mechanical properties of SWNTs of varying size and chirality. We determined the stability domains for circular and collapsed cross section SWNTs. We reported the uniaxial strain–energy behavior of the SWNTs with crossover radius in the range of −8% to 8% strain. The determined structure and lattice parameters for close packed (10, 10)-like nanotubes are in close agreement with observations. We also determined vibrational modes and frequencies of bulk and isolated nanotubes using a highly accurate classical force field. Supplementary material is available at http://www.wag.caltech.edu

References

[1] Iijima S 1991 Helical microtubules of graphitic carbon *Nature* **354** 56–8
[2] Iijima S and Ichlhashi T 1993 Single-shell carbon nanotubes of 1 nm diameter *Nature* **363** 603–5
[3] Bethune D S, Kiang C H, Devries M S, Gorman G, Savoy R, Vazquez J and Beyers R 1993 Cobalt-catalyzed growth of carbon nanotubes with single-atomic-layer walls *Nature* **363** 605–7
[4] Thess A *et al* 1996 Crystalline ropes of metallic carbon nanotubes *Science* **273** 483–7
[5] Krotov Y A, Lee D-H and Louie S G 1997 Low-energy properties of (n, n) carbon nanotubes *Phys. Rev. Lett.* **78** 4245–8
[6] Tuzun R E, Noid D W, Sumpter B G and Merkle R C 1996 Dynamics of fluid-flow inside carbon nanotubes *Nanotechnology* **7** 241–6
[7] Ihara S and Itoh S 1996 Molecular dynamics study of toroidal and helically coiled forms of graphitic carbon *Surf. Rev. Lett.* **3** 827–34
[8] Chopra N G, Benedict L X, Crespi V H, Cohen M L, Louie S G and Zettl A 1996 Fully collapsed carbon nanotubes *Nature* **377** 135–8
[9] Menon M, Richter E and Subbaswamy K R 1996 Structural and vibrational properties of fullerenes and nanotubes in a nonorthogonal tight-binding scheme *J. Chem. Phys.* **104** 5875–82
[10] Hamada N, Sawada S and Oshiyama A 1992 New one-dimensional conductors—graphitic microtubules *Phys. Rev. Lett.* **78** 1579–81
[11] Saito R, Fujita M, Dresselhaus G and Dresselhaus M S 1992 Electronic-structure of chiral graphene tubules *Appl. Phys. Lett.* **60** 2204–6

[12] Blase X, Benedict L X, Shirley E L and Louie S G 1994 Hybridization effects and metallicity in small radius carbon nanotubes *Phys. Rev. Lett.* **72** 1878–81

[13] Robertson D H, Brenner D W and Mintmire J W 1992 Energetics of nanoscale graphitic tubules *Phys. Rev. B* **45** 12 592–5

[14] Yakobson B I, Campbell M P, Brabec C J and Bernholc J 1997 High strain rate fracture and c-chain unraveling in carbon nanotubes *Comput. Mater. Sci.* **8** 341–8

[15] Richter E and Subbaswamy K R 1997 Theory of size dependent resonance raman scattering from carbon nanotubes *Phys. Rev. Lett.* **79** 2738–41

[16] Iijima S, Brabec C, Maiti A and Bernholc J 1996 Structural flexibility of carbon nanotubes *J. Chem. Phys.* **104** 2089–92

[17] Tersoff J and Ruoff R S 1994 Structural properties of carbon nanotube crystals *Phys. Rev. Lett.* **73** 676–9

[18] Ruoff R S, Tersoff J, Lorents D C, Subramoney S and Chan B 1993 Radial deformation of carbon nanotubes by van der Waals forces *Nature* **364** 514–16

[19] Guo Y J 1992 *PhD Dissertation* California Institute of Technology

[20] Guo Y J, Karasawa N and Goddard W A III 1991 Prediction of fullerene packing in C60 and C70 crystals *Nature* **351** 464–7

[21] Gao G, Cagin T and Goddard W A III 1998 Position of K atoms in doped single walled carbon nanotube crystals *Phys. Rev. Lett.* **80** 5056

[22] Lim K T, Brunett S, Iotov M, McClurg R B, Vaidehi N, Dasgupta S, Taylor S and Goddard W A III 1997 Molecular dynamics for very large systems on massively-parallel computers—MPSim program *J. Comput. Chem.* **18** 501–21

[23] Landau L D and Lifshitz E M 1986 *Elasticity Theory* (Oxford: Pergamon)

[24] Rao A M *et al* 1997 Diameter-selective Raman scattering from vibrational modes in carbon nanotubes *Science* **275** 187–91